

# Laser Light-Scattering Characterization of Gelatin in Formamide

CHI WU

Department of Chemistry, The Chinese University of Hong Kong, Shatin, N.T., Hong Kong

## SYNOPSIS

Laser light scattering (LLS) including angular dependence of absolute integrated scattered intensity (static LLS) and of the spectral distribution (dynamic LLS) has been used successfully to characterize gelatin in formamide at room temperature. In static LLS, the use of formamide as a single solvent instead of an aqueous salt solution avoids the well-known problem of preferential sorption of salts in the domain of gelatin molecules. Therefore the true weight-average molecular weight  $M_w$ , the  $z$ -average radius of gyration, and the second virial coefficient have been determined. In dynamic LLS, precise measurements of the intensity-intensity time correlation function permit a Laplace inversion to obtain an estimate of the normalized characteristic linewidth distribution which could be reduced to a translational diffusion coefficient distribution,  $G(D)$ . This report shows that the calibration between  $D$  and  $M$  can be established from  $M_w$  and  $G(D)$  by using only two broadly distributed gelatins instead of a set of narrowly distributed gelatin standards. After establishing a calibration between  $D$  and  $M$ , we were able to estimate the molecular weight distribution of gelatin from  $G(D)$ . © 1994 John Wiley & Sons, Inc.

**Keywords:** laser light scattering • gelatin characterization • molecular weight distribution • calibration between molecular weight and the translational diffusion coefficient

## INTRODUCTION

As an absolute method, laser light scattering (LLS) has been used extensively to characterize polymers. A modern LLS spectrometer can perform both static and dynamic measurements. In static LLS, the angular and concentration dependence of absolute scattered intensity are measured; the weight-average molecular weight ( $M_w$ ), the  $z$ -average radius of gyration ( $\langle R_g^2 \rangle_z^{1/2}$ ), and the second virial coefficient ( $A_2$ ) can be determined from the measured absolute scattered intensities. In dynamic LLS, the intensity-intensity time correlation function is measured. By making a Laplace inversion, we can transform the measured correlation function into a characteristic linewidth distribution ( $G(\Gamma)$ ) which could be reduced further to a translational diffusion coefficient distribution ( $G(D)$ ) or even to a molecular weight distribution (MWD) if we can establish a calibration between  $D$  and  $M$ .

Gelatin forms a class of proteinaceous substances derived from a naturally occurring parent protein, collagen, through some procedures which mostly involve the destruction of the secondary structure of the collagen. Gelatin is well known for its property of forming elastic gels at room temperature in a relatively low concentration: a few percent of gelatin in water. During the gelation process, gelatin molecules renaturalize into a collagen-like structure: a triple-stranded helix. Gelatin has been used widely and extensively in food, photographic, and pharmaceutical industries as an important stabilizer ingredient, such as for pulverulent formulations of vitamin A and carotenoids.<sup>1,2</sup>

Many experimental works related to both the practical use of gelatin and the fundamental aspects implied in the gelation process<sup>1-5</sup> have been performed. Research interests were in the conformational changes of gelatin molecules in solution, the sol-gel transition, and the rheologic properties of gelatin gels over decades.<sup>1-11</sup> In contrast, much less attention has been given to its molecular characterization. This is due mainly to its polyelectrolyte

and polydisperse nature. For example, in size exclusion chromatography (SEC or GPC), besides the calibration problem, it is difficult to find a commercially available ready-to-use column to analyze a broadly distributed gelatin with enough resolution, especially when the weight-average molecular weight is larger than  $3 \times 10^5$  g/mol.

At room temperature, there are two kinds of intermolecular interactions in aqueous gelatin solution. One interaction is the electrostatic interaction because of the presence of electric charges on gelatin (i.e., on the polypeptide chain). The other is the formation of a hydrogen bond between the amino acid units. These interactions have to be eliminated in order to determine the true molecular parameters of gelatin. Adding salts, as in solutions of synthetic polyelectrolytes, is one way to screen the electrostatic interaction and suppress the polyelectrolyte effect. However, most kinds of salts added in aqueous gelatin solution at room temperature will not prevent hydrogen bonding, which is reflected in gelation or in aggregation depending on the gelatin concentration. Only a few salt types (i.e., KSCN and LiBr) are capable of screening off electrostatic interactions and preventing the formation of the hydrogen bond at the same time.

The presence of salts in aqueous gelatin solution creates a problem of preferential sorption of the salt in the domain of gelatin molecules,<sup>1</sup> just as synthetic polyelectrolytes in aqueous salt solutions. In principle, only the apparent molecular parameters can be measured if the sorption is strong. Therefore, in order to obtain the true molecular parameters, the apparent molecular parameters have to be extrapolated to infinitely dilute salt concentration. Even with this time-consuming procedure, there is still no guarantee that the extrapolating values will be the true molecular parameters because the behavior of gelatin in aqueous solution with and without salts could be completely different.

Considering this preferential sorption, some researchers have used nonaqueous solvents, such as formamide, glycerol, and trifluoroethanol, to dissolve gelatin,<sup>12</sup> assuming that those nonaqueous solvents can suppress the above two types of intermolecular interactions. Veis and Anesey<sup>13</sup> investigated the gelatin solutions in formic acid and its mixtures with dimethylformamide at room temperature. Later, Stejskal et al.<sup>14</sup> used formamide as single solvent in static LLS experiments to show that formamide can be used as a solvent for dissolving gelatin at room temperature. It has been suggested that formamide apparently interacts with gelatin by a rather specific, chelated solvation because of similarity between

formamide and gelatin peptide linkages and the known cyclic dimerization of carboxylic acids and amides.<sup>14</sup>

We present the characterization results of two laboratory prepared and one commercial gelatin samples. We show that the calibration between  $D$  and  $M$  can be established by using only two broadly distributed gelatins instead of a set of narrowly distributed gelatin standards. Therefore, in our laser light-scattering characterization of gelatin, not only  $M_w$ ,  $\langle R_g^2 \rangle_z^{1/2}$  and  $A_2$ , but also an estimate of  $G(D)$  and MWD of gelatin, are obtained.

## EXPERIMENTAL

### Solution Preparation

Two laboratory prepared gelatins are courtesy of Dr. Klaus Bräumer and Dr. Wilfried Babel (DGF, Deutsche Gelatine-Fabriken Stoess AG, Eberbach). One is A-type (Bloom value 310, Batch #: 50100) and the other is B-type (Bloom value 200, Batch #: 21020). They are denoted hereafter as gelatin-A and gelatin-B, respectively. The third gelatin (Bloom value 200, 176497) is a commercial product of DGF. Formamide is obtained from BASF AG (Germany, analytical grade, 99.5%). The gelatins and formamide were used without further purification. Gelatin solutions of 1–5 mg/mL were prepared by dissolving a determined amount of gelatin in formamide first at 50°C for 1 hour and then maintaining them at room temperature for at least one day. An estimate of 12% water in gelatin was taken into account when we calculated the final gelatin concentration. All solutions were clarified with a 0.22  $\mu\text{m}$  Millipore filter in order to remove dust.

### Laser Light Scattering

Intensities of light scattered from the gelatin solutions at different scattering angles (30–90°) were measured with a commercial LLS spectrometer (ALV/SP-86, Germany). An Argon ion laser (Coherent INNOVA 300, operated at wavelength 488 nm and 300 mw) was used as the light source. The primary beam is vertically polarized. By placing a polarizer in front of the detector, we measured only the vertically polarized scattered light. An ALV-3000 correlator with 240 linear channels was used to measure the intensity–intensity time correlation functions. All LLS measurements were performed at 25°C.

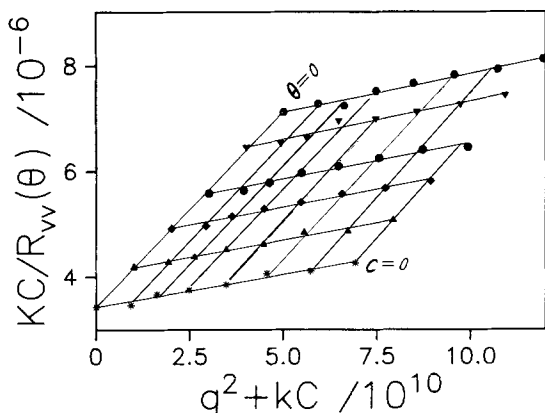


**Figure 1.** Typical Zimm plot of gelatin B in formamide at 25°C, where the gelatin concentration is 1–5 mg/mL and the scattering angle is 30–90°.

## RESULTS AND DISCUSSION

### Light-Scattering Intensity Measurements

The angular dependence of the excess absolute time-averaged scattered intensity, known as the excess Rayleigh ratio [ $R_{vv}(\theta)$ ], was measured. For a dilute polymer solution at concentration  $C$  (g/mL) and scattering angle  $\theta$ ,  $R_{vv}(\theta)$  can be approximately expressed as<sup>15</sup>

$$\frac{KC}{R_{vv}(\theta)} \cong \frac{1}{M_w} \cdot \left(1 + \frac{1}{3} \langle R_g^2 \rangle_z q^2\right) + 2A_2 C \quad (1)$$

where  $K = 4\pi^2 n^2 \left(\frac{\partial n}{\partial C}\right)^2 / (N_A \lambda_0^4)$  with  $N_A$ ,  $n$ , and  $\lambda_0$  being Avogadro's number, the solvent refractive index, and the wavelength of light in vacuo, respec-

tively, and  $q = \frac{4\pi n}{\lambda_0} \sin\left(\frac{\theta}{2}\right)$ . By measuring  $R_{vv}(\theta)$  at different  $C$  and  $\theta$ , we can determine  $M_w$ ,  $\langle R_g^2 \rangle_z^{1/2}$ , and  $A_2$  from the Zimm plot which incorporates  $\theta$  and  $C$  extrapolations on a single grid.

Figure 1 shows a typical Zimm plot of gelatin B in formamide at 25°C. Based on eq. (1), we can determine:  $\langle R_g^2 \rangle_z^{1/2}$  from the slope of  $\left(\frac{KC}{R_{vv}(\theta)}\right)_{C=0}$  versus  $q^2$ ;  $A_2$  from the slope of  $\left(\frac{KC}{R_{vv}(\theta)}\right)_{\theta=0}$  versus  $C$ ; and  $M_w$  from the intercept of  $\left(\frac{KC}{R_{vv}(\theta)}\right)_{C=0, \theta=0}$

They are listed in Table I. The positive values of  $A_2$  show that formamide is a good solvent for dissolving gelatin at room temperature.

### Light-Scattering Linewidth Measurements

The measured intensity–intensity time correlation function  $G^{(2)}(n\Delta\tau, \theta)$  in the self-beating mode has the form<sup>16</sup>

$$G^{(2)}(n\Delta\tau, \theta) = A[1 + \beta |g^{(1)}(n\Delta\tau, \theta)|^2] \quad (2)$$

where  $A$  is the measured baseline,  $\beta$  is a parameter depending on the coherence of the detection,  $n$  is the channel number,  $\Delta\tau$  is the sample time, and  $g^{(1)}(n\Delta\tau, \theta)$  is the first-order electric field correlation function. In our correlation function measurements, the accumulated photon counts in each channel were more than  $10^6$  so that the statistic noise is less than 0.1%. In addition, we do not use  $A$  as an adjustable parameter and insist on having

**Table I.** Static and Dynamic LLS Results of Gelatins in Formamide at 25°C

Gelatin	$\frac{10^{-5}M_w}{\text{mol}^{-1} \text{g}}$	$\frac{\langle R_g^2 \rangle_z^{1/2}}{\text{nm}}$	$\frac{10^{-4}A_2}{\text{g}^{-2} \text{mol} \cdot \text{mL}}$	$\frac{10^{-8}\bar{D}}{\text{cm}^2 \text{ s}^{-1}}$	$\frac{R_h}{\text{nm}}$	$\frac{k_d}{\text{g}^{-1} \text{ mL}}$	$f$
A	2.92	33	3.7	3.58	18.0	35	0.15
B	3.71	38	6.2	3.11	20.5	63	0.17
176497	3.46	37	4.5	3.24	19.8	50	0.16

The following  $M_z$ ,  $M_w$ , and  $M_n$  were obtained from dynamic LLS where the calibration of  $D = 5.98 \times 10^{-5} \text{M}^{-0.58}$  was used:

Gelatin	$\frac{10^{-6}M_z}{\text{mol}^{-1} \text{g}}$	$\frac{10^{-5}M_z}{\text{mol}^{-1} \text{g}}$	$\frac{10^{-5}M_n}{\text{mol}^{-1} \text{g}}$	$M_w : M_n$
A	8.30	3.61	1.57	2.3
B	1.56	3.00	1.65	1.8
176497	3.86	3.48	1.32	2.7

$A$  and  $\lim_{n \rightarrow \infty} G^{(2)}(n\Delta\tau, \theta)$  (the calculated baseline) agree to within 0.1%. For a polydisperse sample,  $g^{(1)}(n\Delta\tau, \theta)$  is related to the normalized characteristic linewidth distribution  $G(\Gamma)$ :

$$g^{(1)}(n\Delta\tau, \theta) = \int_0^\infty G(\Gamma) e^{-\Gamma n\Delta\tau} d\Gamma \quad (3)$$

We have used two established methods to analyze the correlation function profile:

### Cumulants Expansion<sup>17</sup>

$$\ln |g^{(1)}(n\Delta\tau, \theta)| = -\bar{\Gamma}n\Delta\tau + \frac{1}{2}\mu_2(n\Delta\tau)^2 + \frac{1}{6}\mu_3(n\Delta\tau)^3 + \dots \quad (4)$$

where  $\bar{\Gamma} = \int_0^\infty \Gamma G(\Gamma) d\Gamma$  and  $\mu_m = \int_0^\infty (\Gamma - \bar{\Gamma})^m G(\Gamma) d\Gamma$ . The variance,  $\mu_2/\bar{\Gamma}^2$ , characterizes the distribution width. The cumulants method is applicable as long as  $G(\Gamma)$  is not too broad;

### Laplace Inversion of Eq. (3)

We used the analysis program CONTIN<sup>18</sup> which was kindly furnished by S. W. Provencher.

Figure 2 shows a typical intensity-intensity time correlation function of gelatin A where  $\theta = 90^\circ$  and  $C = 1.00 \times 10^{-3}$  g/mL. The same correlation function was analyzed by using the second-order cumulant fit, the third-order cumulant fit, and CONTIN. The calculated values of  $\bar{\Gamma}$  are 3.36, 3.80, and  $3.95 \times 10^{-8}$  cm<sup>-2</sup>/s, respectively. The third-order cumulant fit and CONTIN give essentially the same

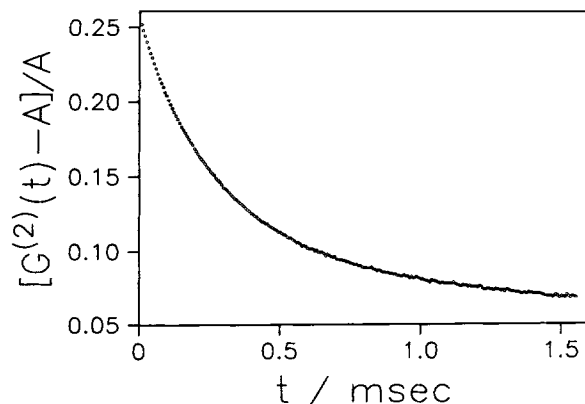


**Figure 2.** Typical intensity-intensity time correlation function of gelatin A in formamide at 25°C, where  $C = 1.00 \times 10^{-3}$  g/mL and  $\theta = 90^\circ$ .

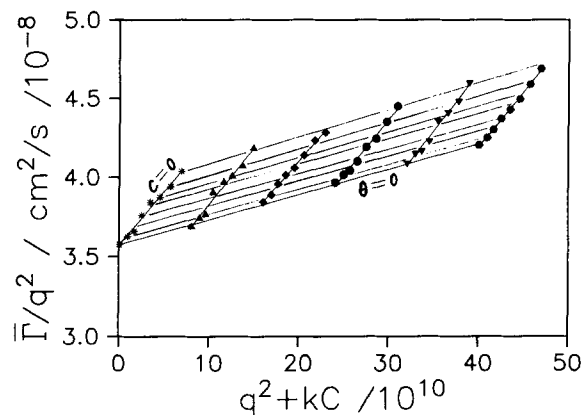


**Figure 3.**  $\bar{\Gamma}/q^2$  of gelatin B at 25°C as a function of  $q$  and  $C$ , where  $C$  and  $\theta$  are the same as in Figure 1.  $\bar{\Gamma}$  was calculated by using a third-order cumulants fit.

average results; the second-order cumulant fit is not a proper method in this case because gelatin is broadly distributed. In comparison with CONTIN, the third-order cumulant fit requires much less computer time. The relative fitting errors for all channels are usually less than 5%.

In general,  $\bar{\Gamma}$  is a function of both  $C$  and  $\theta$ . As  $C$  increases, the interactions between polymer molecules will affect the diffusion process, which is normally a linear function of  $C$  when solution is dilute. On the other hand, as  $\theta$  increases, the internal molecular motions will influence  $\bar{\Gamma}$ . The effects can be expressed in the form<sup>19</sup>

$$\frac{\bar{\Gamma}}{q^2} = \bar{D}(1 + k_d C)(1 + f \langle R_g^2 \rangle_z q^2) \quad (5)$$

where  $k_d$  is the diffusion second virial coefficient;  $f$ , a dimensionless number which depends on chain structure, polydispersity, and solvent quality. The theoretical values of  $f$  for a number of Gaussian models (linear and branched) are known.<sup>20-22</sup> For monodisperse linear chains,  $f = 13/75$  without preaveraging and  $f = 2/15$  with preaveraging. For polydisperse linear chains with a Flory's "most probable" distribution, the corresponding values rise to 0.2 and 0.1667, respectively. In general, branching will lower the value of  $f$ .

Figure 3 shows a typical plot of  $\bar{\Gamma}/q^2$  versus  $(q^2 + k \cdot C)$  of gelatin B in formamide at 25°C. It is very similar to the Zimm plot in static LLS data analysis. Based on eq. (5), we can determine  $f \langle R_g^2 \rangle_z$  from the slope of  $(\bar{\Gamma}/q^2)_{C=0}$  versus  $q^2$ ;  $k_d$  from the slope of  $(\bar{\Gamma}/q^2)_{\theta=0}$  versus  $C$ ; and  $\bar{D}$  from the intercept of

$(\bar{\Gamma}/q^2)_{C=0, \theta=0}$ .  $f$  can be further calculated from  $f \langle R_g^2 \rangle_z$  if we use the value of  $\langle R_g^2 \rangle_z$  from static LLS.  $\bar{D}$  can be further related to the hydrodynamic radius  $R_h$  by using the Stokes-Einstein equation:

$$R_h = \frac{k_B T}{6\pi\eta\bar{D}}$$

with  $k_B$ ,  $T$ , and  $\eta$  being the Boltzmann constant, the experimental temperature, and the viscosity of formamide, respectively. The calculated values of  $\bar{D}$ ,  $R_h$ ,  $k_d$ , and  $f$  are also listed in Table I. The positive values of  $k_d$  confirm that formamide is indeed a good solvent for dissolving gelatin at room temperature. It is interesting to find that the values of  $f$  are very close to the ones predicted for a random-coil in good solvent. The ratio of  $\langle R_g^2 \rangle_z^{1/2}/R_h$  is also a very important parameter which does not depend on the bond length and the molecular weight, but on the polymer architecture, the chain conformation, and polydispersity. For a monodisperse and polydisperse ( $M_w/M_n = 2.0$ ) linear polymer coil, the ratios of  $\langle R_g^2 \rangle_z^{1/2}/R_h$  are 1.504 and 1.732, respectively.<sup>23-25</sup> The values of  $\langle R_g^2 \rangle_z^{1/2}/R_h$  for gelatin in formamide is about 1.84, which shows that gelatin is a broadly distributed linear polymer and the gelatin chain in formamide at room temperature behaves, more or less, like a random coil.

### Transformation of $G(D)$ to MWD

With the calculated  $k_d$ ,  $\langle R_g^2 \rangle$ , and  $f$ , we can easily transform  $G(\Gamma)$  at  $C$  and  $\theta$  into a translational diffusion coefficient distribution  $G(D)$  at  $C = 0$  and  $\theta = 0$  according to eq. (5).

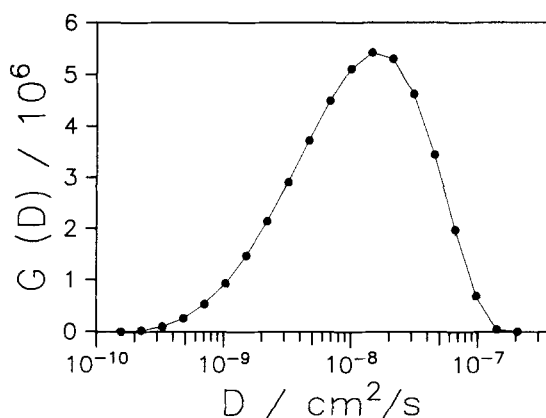


**Figure 4.** Typical translational diffusion coefficient distribution  $G(D)$  of gelatin A in formamide at 25°C.

Figure 4 shows a typical  $G(D)$  of gelatin A in formamide at 25°C, where CONTIN was used to obtain  $G(D)$  from the correlation function. The values of  $\bar{D}$  and  $\mu_2/\bar{D}^2$  are  $3.23 \times 10^{-8}$  cm<sup>2</sup>/s and 0.5, respectively. In order to transform  $G(D)$  to a molecular weight distribution (MWD), we have to establish a calibration between  $D$  and  $M$ , i.e.,

$$D = k_D M^{-\alpha_D} \quad (6)$$

where  $k_D$  and  $\alpha_D$  are two calibration constants. If knowing  $k_D$  and  $\alpha_D$ , we can transform  $G(D)$  to MWD according to the following principles: at  $C = 0$  and  $\theta = 0$ , we have

$$\int_0^\infty G(D) dD = \gamma \int_0^\infty F_z(M) dM \quad (7)$$

where  $\gamma$  is a normalization constant and  $F_z(M) = MF_w(M) = M^2 F_n(M)$  with the subscripts  $z$ ,  $w$ , and  $n$  meaning intensity, weight, and number distribution of molecular weight, respectively. After combining eq. (6) and (7), we obtain

$$\begin{aligned} \int_0^\infty \alpha_D \cdot D \cdot G(D) d[\ln(M)] \\ = \gamma \cdot \int_0^\infty M \cdot F_z(M) d[\ln(M)] \end{aligned} \quad (8)$$

By comparing the left side of eq. (8) with the right side, we have

$$F_z(M) = \frac{\alpha_D \cdot D \cdot G(D)}{\gamma M} \quad (9)$$

In eq. (9) we have taken the integrand as one way to represent the same polymer distribution. Based on eqs. (6) and (9), we can use  $G(D)$  to calculate  $F_z(M)$ ,  $F_w(M)$ , and  $F_n(M)$  if  $k_D$  and  $\alpha_D$  are known, where  $\gamma$  as a constant is irrelevant to the distribution. In order to compare the calculated molecular weight distribution with the results from static LLS, we should further calculate  $M_w$  from  $G(D)$ . Based on the definition of  $M_w$ , we have

$$M_w = \frac{\int_0^\infty F_w(M) M dM}{\int_0^\infty F_w(M) dM} \quad (10)$$

It is easy to rewrite eq. (11) as

$$M_w = \frac{\int_0^\infty F_z(M) dM}{\int_0^\infty F_z(M)/M dM} \quad (11)$$

By combining eqs. (6), (9), and (11), we can calculate  $M_w$  from  $G(D)$  by using

$$(M_w)_{\text{calcd}} = \frac{k_D^{1/\alpha_D} \int_0^\infty G(D) dD}{\int_0^\infty G(D) D^{1/\alpha_D} dD} \quad (12)$$

In the past, several methods have been used to find  $k_D$  and  $\alpha_D$ , such as measuring  $\bar{D}$  and  $M_w$  for a set of narrowly distributed standards<sup>26</sup> and estimating the calibrating constant from other experimental results (e.g., from polymer conformation, solvent quality, and viscosity data).<sup>27</sup> Unfortunately, it is difficult in practice to have a set of narrowly distributed gelatin standards with different molecular weights. Based on the values of  $\bar{D}$  and  $M_w$  of gelatin A and gelatin B in Table I, we obtain:  $\bar{k}_D = (5.09 \pm 0.50) \times 10^{-5}$  and  $\bar{\alpha}_D = 0.577 + 0.010$ , where “-” emphasizes that they are obtained from  $\bar{D}$  and  $M_w$ . However, the calculated  $M_w$  from  $G(D)$  for gelatin A ( $2.41 \times 10^5$  g/mol) and gelatin B ( $2.91 \times 10^5$  g/mol) with  $\bar{k}_D$  and  $\bar{\alpha}_D$  are too small in comparison with  $M_w$  listed in Table I. This difference is understandable since  $\bar{D}$  and  $M_w$  are respectively different from  $D$  and  $M$  for a polydisperse sample.

In order to find correct  $\alpha_D$  and  $k_D$  without using

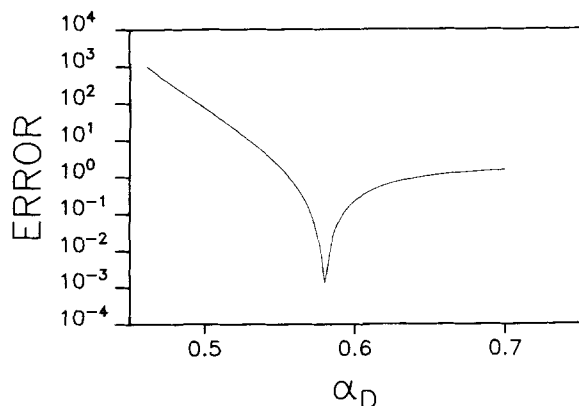


**Figure 5.** Typical plot of ERROR versus  $\alpha_D$  (see text for the definition of ERROR). The minimum corresponds to  $\alpha_D = 0.580$ .

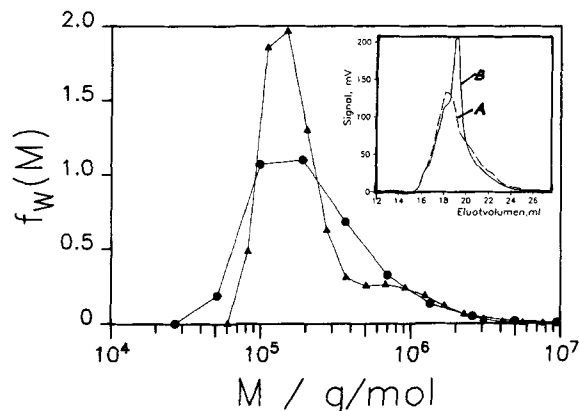


**Figure 6.** Normalized weight distributions,  $f_w(M)$ , of gelatin A (circles) and gelatin B (triangles). The inset shows the SEC elution curves of these two gelatins.

a set of narrowly distributed standards, we have used the following principles: for two samples, we have two measured  $M_w$  from static LLS and two calculated  $G(D)$  from dynamic LLS, denoted as  $M_{w,1}$ ,  $M_{w,2}$ ,  $G_1(D)$  and  $G_2(D)$ . We also have two  $(M_w)_{\text{calcd}}$  based on eq. (12), denoted as  $(M_{w,1})_{\text{calcd}}$  and  $(M_{w,2})_{\text{calcd}}$ . The ratio of  $(M_{w,1})_{\text{calcd}}$  and  $(M_{w,2})_{\text{calcd}}$  is

$$\frac{(M_{w,1})_{\text{calcd}}}{(M_{w,2})_{\text{calcd}}} = \frac{\left[ \int_0^\infty G_1(D) dD \right] \left[ \int_0^\infty G_2(D) D^{1/\alpha_D} dD \right]}{\left[ \int_0^\infty G_2(D) dD \right] \left[ \int_0^\infty G_1(D) D^{1/\alpha_D} dD \right]} \quad (13)$$

Two calculated  $(M_w)_{\text{calcd}}$  should equal the two measured  $M_w$ , which means that the left side of eq. (13) can be replaced by the ratio of  $M_{w,1}/M_{w,2}$ . Thus, there is only one unknown parameter  $\alpha_D$  in eq. (13). In practice, by iterating  $\alpha_D$ , we will be able to find a proper  $\alpha_D$  which minimizes the difference between both sides of eq. (13). With this,  $\alpha_D$ , we can further determine the value of  $k_D$  from  $M_w$  and  $G(D)$  by using eq. (12). Now we ask whether  $\alpha_D$  and  $k_D$  calculated in this way are well defined.

Figure 5 shows the relative ERROR versus  $\alpha_D$ , where ERROR has been defined as

$$\text{ERROR} = \left[ \frac{(M_{w,1})_{\text{calcd}} - M_{w,1}}{M_{w,1}} \right]^2 + \left[ \frac{(M_{w,2})_{\text{calcd}} - M_{w,2}}{M_{w,2}} \right]^2 \quad (14)$$

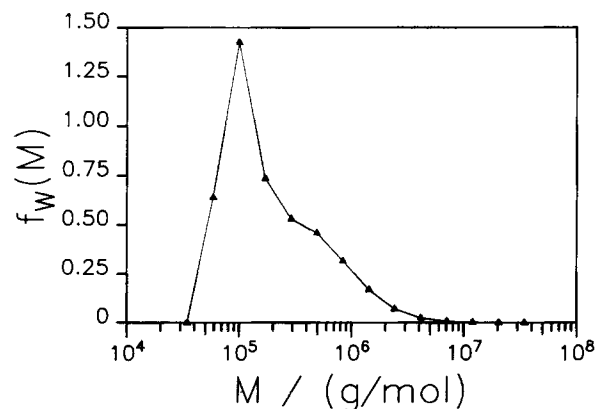
and  $k_D = 5.98 \times 10^{-5}$ . It is clear that ERROR increases sharply if  $\alpha_D$  is deviated from 0.580. After comparing  $k_D$  and  $\alpha_D$  with the previous calculated  $\bar{k}_D$  and  $\bar{\alpha}_D$ , we find that  $\alpha_D$  is essentially the same as  $\bar{\alpha}_D$  and  $k_D$  is  $\sim 20\%$  larger than  $\bar{k}_D$ . By using the calculated  $k_D$  ( $=5.98 \times 10^{-5}$ ) and  $\alpha_D$  ( $=0.580$ ), we were able to calculate the molecular weight distributions of gelatin A and gelatin B.

Figure 6 shows the normalized weight distributions of molecular weight,  $f_w(M)$ , of gelatin A (circles) and gelatin B (triangles). Based on these two distributions, we were able to calculate  $M_z$ ,  $M_w$ , and  $M_n$ , which are summarized in Table I.

In practice, size exclusion chromatography (SEC) is a more established method for the characterization of molecular weight distribution. For comparison, the SEC elution curves of gelatin A and gelatin B are also presented in Figure 6 (inset). It shows that the molecular weight distributions obtained from our LLS measurements are similar to the distributions obtained from SEC measurements: gelatin A is broader and gelatin B is bimodal. Unfortunately, direct comparison of the molecular weight distributions obtained from LLS with those from SEC is not feasible at the present time because it is very difficult to obtain an absolute calibration of our SEC columns for gelatin characterization.

Further, by using the known values of  $k_d$ ,  $f$ ,  $k_D$ , and  $\alpha_D$ , we are able to determine the molecular weight distribution of gelatin from only *one* measured translational diffusion coefficient distribution of a dilute gelatin solution at only *one* scattering angle.

Figure 7 shows  $f_w(M)$  of a commercial gelatin (B 200, 176497), which was obtained by measuring one solution (1.00 g/mL) at one angle ( $90^\circ$ ). The cal-



**Figure 7.** Normalized weight distribution  $f_w(M)$  of a commercial gelatin (B 200, 176497).

culated  $M_z$ ,  $M_w$ , and  $M_n$  of this gelatin are also listed in Table I. The calculated  $M_w$  are confirmed by the measured one from our static light scattering. The larger value of  $M_w/M_n$  ( $=2.7$ ) shows that its distribution is more broad in comparison with the two laboratory prepared gelatin samples.

Finally, we should state that the profile of  $f_w(M)$  calculated from  $G(D)$  is only an estimation of molecular weight distribution since the inversion of eq. (3) is a well-known ill-conditioned problem. The relative errors of  $f_w(M)$ , especially at both the low and high molecular weight ends, could be as high as 20%. However, the calculated average values of  $\bar{D}$  and  $(M_w)_{\text{calcd}}$  are quite stable and the typical relative errors are less than 5%.

## CONCLUSIONS

We have accomplished the characterization of gelatin in formamide at room temperature by using laser light scattering. It is confirmed that formamide is a good solvent for dissolving gelatin at room temperature. Our experimental results suggest that the gelatin chain in formamide at room temperature is flexible and has a random coil conformation. After establishing a calibration between the translational diffusion coefficient and the molecular weight by using only two broadly distributed gelatins, we are able to determine not only the weight-average molecular weight, but also an estimate of the molecular weight distribution. The calibration is independent on our particular LLS as long as formamide is used as solvent and temperature is  $25^\circ\text{C}$ . With this calibration, dynamic light scattering becomes a good, absolute method for the characterization of the molecular weight distribution of gelatin even if it does not have the same resolution as SEC. The second virial coefficient reported here enables us to characterize gelatin with only one concentration in the future. As a good solvent, formamide can also be used in other solution methods to characterize gelatin.

The author is indebted to Mr. Kern for performing the LLS experiments and Mr. Werle for preparing the figures.

## REFERENCES AND NOTES

1. A. G. Ward and A. Courts, *The Science and Technology of Gelatin*, Academic Press, London, 1977.
2. A. Veis, *The Macromolecular Chemistry of Gelatin*, Academic Press, London, 1964.

3. M. Djabourov, *Contemp. Phys.*, **29**(3), 273 (1988).
4. M. E. Newcomer, T. A. Jones, J. Aqvist, J. Sundelin, U. Eriksson, L. Rask, and P. A. Peterson, *EMBO J.*, **3**(7), 1451 (1984).
5. C. Quellet, H. F. Eicke, R. Gehrke, and W. Sager, *Europhys. Lett.*, **9**(3), 293 (1989).
6. W. Borchard, B. Luft, and P. Reutner, *J. Photogr. Sci.*, **34**(4), 132 (1986).
7. W. Borchard, K. Bergmann, A. Emberger, and G. Rehage, *Prog. Colloid Polym. Sci.*, **60**, 120 (1976).
8. M. Djabourov and P. Papon, *Polymer*, **24**, 537 (1983).
9. H. Yoon, H. Kim, and H. Yu, *Macromolecules*, **22**, 848 (1989).
10. T. Change and H. Yu, *Macromolecules*, **17**, 115 (1984).
11. P. S. Russo, M. Mustafa, D. Tipton, N. Nelson, and D. Fontenot, *Polym. Mater. Sci. Eng.*, **59**, 605 (1988).
12. J. Q. Umberger, *Photographic Sci. & Eng.*, **11**(6), 385 (1967).
13. A. Veis and J. Anesey, *J. Phys. Chem.*, **63**, 1720 (1959).
14. J. Stejskal, D. Straková, and P. Kratochvil, *Makromol. Chem.*, **188**, 855 (1987) and references therein.
15. B. Chu, *Laser Light Scattering*, Academic Press, New York, 1974.
16. R. Pecora, *Dynamic Light Scattering*, Plenum Press, New York, 1975, p. 217.
17. D. E. Koppel, *J. Chem. Phys.*, **57**, 4814 (1972).
18. S. W. Provencher, *Biophys. J.*, **16**, 29 (1976); *J. Chem. Phys.*, **64**, 2772 (1976); *Makromol. Chem.*, **180**, 201 (1979).
19. W. H. Stockmayer and M. Schmidt, *Pure Appl. Chem.*, **54**, 407 (1982); *Macromolecules*, **17**, 509 (1984).
20. A. Z. Akcasu, M. Benmouna, and C. C. Han, *Polymer*, **21**, 866 (1980).
21. W. Burchard, M. Schmidt, and W. H. Stockmayer, *Macromolecules*, **13**, 580; **13**, 1265 (1980).
22. H. Yamakawa, *Modern Theory of Polymer Solutions*, Harper & Row, New York, 1971.
23. K. Huber, S. Bantle, P. Lutz, and W. Burchard, *Macromolecules*, **18**, 1461 (1985).
24. A. Z. Akcasu and C. C. Han, *Macromolecules*, **12**, 276 (1979).
25. E. Nordmeier and D. Lechner, *Polym. J.*, **21**(8), 623 (1989).
26. B. Chu, C. Wu, and J. R. Ford, *J. Colloid Interface Sci.*, **105**, 473 (1985).
27. J. W. Pope and B. Chu, *Macromolecules*, **17**, 2633 (1984).

Received March 22, 1993

Revised August 31, 1993

Accepted September 1, 1993